Journal of Engineering Technology and Applied Physics

Rice Leaf Nitrogen Content Estimation Through A Methodological Framework Using Single-Sensor Multispectral Images

Muliady Ang[1, 2], Lim Tien Sze[2, *], Koo Voon Chet[2], Dimitri Jeremy[1] and Eric Chandra[1]
[1]*Electrical Engineering Department, Universitas Kristen Maranatha, Bandung, Indonesia.*
[2]*Faculty of Engineering and Technology, Multimedia University, Melaka, Malaysia.*
**Corresponding author:* tslim@mmu.edu.my, *ORCiD:* 0000-0002-7899-8750
https://doi.org/10.33093/jetap.2024.6.2.6
Manuscript Received: 29 December 2023, Accepted: 18 March 2024, Published: 15 September 2024

***Abstract* — Using non-destructive evaluation tools based on imaging techniques, including single-sensor multispectral cameras, provides a cost-effective solution for optimizing rice nitrogen fertilization through site-specific nutrient management. However, their accuracy and precision have been identified as areas for improvement. This study aims to develop a methodology to improve the accuracy of estimations through field experiments. It utilizes multispectral images captured by MAPIR Survey3W Orange Cyan Near-Infrared and MAPIR Survey3W Red Edge cameras. The Normalized Difference Vegetation Index and Red Edge values derived from these images are correlated with Soil Plant Analysis Development values to assess rice nitrogen levels. A prediction model is then built using the Support Vector Regression algorithm. Findings from the experiments underscore the importance of addressing shadow effects, integrating the dataset on light intensity and image capture time, conducting radiometric calibration, filtering outlier data, employing image segmentation, and utilizing nonlinear Canova tests to enhance estimation accuracy. By configuring the Support Vector Regression model with RBF kernel, gamma set to 1.24, and epsilon set to 0.1, the R2 of the train data and validation data reaches 0.851, and 0.840 respectively. Meanwhile, the R2 of the test data achieves 0.793 with a mean absolute percentage error of 3.49% and a root mean square error of 1.70. These findings underscore the potential of the proposed methodology to improve the estimation of rice nitrogen status based on single-sensor multispectral images, paving the way for more effective nutrient management strategies in rice cultivation.**

***Keywords*—Single-sensor multispectral images, Rice leaf nitrogen content, Framework, Super Vector Regression.**

I. INTRODUCTION

Meeting the nutritional requirements of populations is imperative in numerous regions worldwide, where staples such as grains, legumes, and root crops constitute the primary source of calories, protein, and essential nutrients essential for maintaining optimal health. Regrettably, the surge in global food demand has been met with significant disruptions in food production due to a multitude of factors. These include climate change, limited resource availability, geopolitical conflicts, humanitarian crises, natural disasters, evolving population dynamics, producer and consumer behaviors, trade dynamics, and policy responses [1]. The COVID-19 pandemic, a prevailing global crisis, has unveiled substantial dangers that imperil both the availability and stability of food systems, thereby jeopardizing global food security [2]. Food security remains a paramount concern for certain East and Southeast Asian countries, particularly concerning rice production, a staple crop in these regions. The adverse effects of climate change on rice cultivation [3] necessitate urgent attention to address the prevalent yield gap. Bridging this gap, which denotes the disparity between current production levels and the maximum potential yield, is imperative to sustain Southeast Asia's position as a preeminent rice-producing region [4].

Given the constraints of limited land availability and the imperative to enhance rice production, farmers are increasingly turning to intensification farming systems. These systems are designed to maximize productivity through the implementation of various approaches, including precision agriculture, which leverages technologies such as Global Positioning System (GPS) and sensors to optimize the application of fertilizers, water, and pesticides. Intensification also

encompasses the adoption of high-yielding crop varieties, improved irrigation methods, mechanization, and the utilization of modern farming techniques. Nevertheless, it is crucial to strike a balance between intensification efforts and sustainable practices to mitigate adverse environmental impacts, such as soil degradation, water pollution, and loss of biodiversity [5]. Crop management practices are implemented to meet the demands of intensive rice production and future rice needs through the adoption of knowledge-based strategies that prioritize the efficient utilization of all inputs, including fertilizer management [6].

Nitrogen (N) plays a pivotal role in the growth, development, and yield formation of rice plants, underscoring the significance of enhancing nitrogen use efficiency (NUE) to optimize agricultural productivity. Agronomic approaches are employed to improve NUE, encompassing techniques like screening rice varieties with superior N utilization, innovating and utilizing N fertilizers, optimizing the timing and methods of fertilization, employing nitrification and urease inhibitors to enhance N availability, and promoting the adoption of fertilizer-saving technologies. These strategies aim to maximize the effectiveness of N fertilization, minimize losses, and enhance overall NUE in rice cultivation [7].

One widely recognized practice is site-specific nutrient management (SSNM), which integrates various methodologies such as soil testing, crop nutrient uptake models, precision agriculture technologies, and agronomic expertise. SSNM highlights the significance of adopting a precise and targeted approach to fertilizer management, rather than relying on generalized recommendations [8]. The implementation of SSNM involves dynamic adjustment of N rates in agriculture, which entails adapting the application of N fertilizers based on real-time or near real-time information about crop growth, nutrient availability, and environmental conditions. Several tools can facilitate the dynamic adjustment of N rates, including the leaf color chart (LCC) and soil plant analysis development (SPAD) meter [9]. Modern electronic and computing technology development makes significant contributions to analyzing and measuring the rice N status, for example:

- Optical Sensors or Cameras

Visual, multispectral, or hyperspectral images can be used for calculating vegetation indices (VI's), such as normalized difference vegetation index (NDVI) or canopy reflectance. These VIs provide information on crop health and vigor, allowing farmers to adjust N rates accordingly. Optical sensor data can be used to estimate crop leaf N content and guide variable rate N application [10, 11].

- Crop Models and Decision Support Systems

Mathematical models and decision support systems can integrate various data inputs, such as weather data, soil characteristics, and crop growth parameters, to simulate crop nutrient requirements and predict optimal N rates. These tools enable farmers to make informed decisions regarding N fertilization based on specific field conditions and crop growth stages [12].

- Mobile Applications and Data Analytics

Mobile applications and digital platforms can facilitate data collection, storage, and analysis for N rate adjustment. These tools can integrate field-specific data, including soil test results, weather data, and crop monitoring data, to provide real-time recommendations for N rate adjustments [13].

- Remote Sensing and Satellite Imagery

Satellite imagery and aerial remote sensing can provide valuable information on crop growth and nutrient status. These tools allow for the monitoring of VI, biomass accumulation, and canopy health over large areas, aiding in the adjustment of N rates based on spatial variations within a field [14, 15].

Checking N levels in rice is essential in SSNM practice, so a current study on assessing rice N content is needed. In general, there will be a need for improved sensing systems that are more dependable, precise, durable, and cost-effective in various aspects of crop production. These advancements will enable better and more efficient site-specific management of specialty crops. However, there are still many challenges to overcome due to the complex and unstructured nature of the agricultural environment [16]. Optical sensors have become a popular choice for this purpose because of their non-destructive, easy, and fast process of measurement. Especially in estimating the rice leaf N content based on a hyperspectral camera [17] or multispectral camera [18]. In general, hyperspectral and multispectral cameras provide notable benefits over visual cameras in estimating N levels in rice [11]. These advantages stem from their enhanced spectral information, improved precision, early detection of deficiencies, and potential for advanced data analysis and modeling. These combined advantages contribute to the enhancement of N management in rice farming, resulting in better crop yields and optimized utilization of resources. However, the price of hyperspectral cameras is expensive, ranging from thousands to tens of thousands of dollars, and high-end multispectral cameras that use multi-sensors also cost a lot. This is the main obstacle to application in the field, especially for farmers in developed countries. Recently, a multispectral camera using only one sensor at a relatively affordable price has been launched, but it has many weaknesses, especially leading to reduced spectral resolution and accuracy compared to using multiple-sensor cameras. This is due to the limited capacity of a single sensor to accurately detect and distinguish between various wavelengths of light, and environmental uncertainty [19, 20]. Consequently, the task at hand is quite challenging, as numerous problematic issues become evident when examining images of crops. This paper emphasizes a methodology framework to estimate the rice leaf N content using a single-sensor multispectral camera

(SSMC) based on the field experiment. The goal is to give a comprehensive guide, and the practice should be considered when using a SSMC for estimating the rice leaf N content.

II. METHODOLOGY

Efforts to leverage multispectral images acquired from low-cost cameras with a single sensor to estimate rice leaf N content have primarily focused on exploring modeling algorithms, particularly employing machine learning techniques to enhance estimation accuracy [21]. However, often overlooked or inadequately addressed are other critical processes such as camera selection, image capture, and data collection techniques, as well as image and data preprocessing, despite their significant impact on the quality of training data, which directly affects the prediction model. In general, the estimation of rice leaf N content using a multispectral camera involves analyzing the reflectance values of the rice leaf and applying suitable algorithms. In the previous study that used only the NDVI value, the prediction model's performance R2 only reached 0.51. In this study, the Red Edge (RE) and NDVI values were mapped to the SPAD value by computing the reflectance of rice leaves to create a more accurate model. This research utilized two MAPIR Survey3 cameras to capture RE spectral, and Orange+Cyan+Near-Infrared (OCN) spectral. OCN images are known for providing improved contrast in NDVI images between the soil and plants compared to the Red+Green+Near-Infrared (RGN) camera. The OCN camera model captures light at specific wavelengths: Near-Infrared at 808nm, Orange at 615 nm, and Cyan at 490 nm [22]. By considering these factors, this work aims to enhance the accuracy and reliability of the prediction model for rice leaf N content. This research delineated five fundamental steps involved in constructing a prediction model for rice leaf N content using an SSMC described below:

- Data and image collection: Gather a dataset of rice plants with known N content. This data should include both spectral measurements and the corresponding N content determined through a SPAD meter, as well as the other features needed. Use the multispectral camera to capture images of the rice plants. Ensure that the lighting conditions are consistent and correct exposure during image capture to maintain data quality.

- Data cleaning and image preprocessing: Preprocess the captured multispectral images to correct for any distortions, such as radiometric calibration and geometric corrections. And then conduct a series of data-cleaning steps. This stage is essential to ensuring an accurate and unbiased dataset.

- Extract spectral information: Extract the spectral information from the multispectral images. This involves analyzing the reflectance values of the rice plants at different spectral bands and calculating the NDVI and RE values.

- Develop a prediction model: Use the collected data to develop a prediction model. Apply a machine learning algorithm to establish a relationship between the features (NDVI and RE values) and the output SPAD values. Various algorithms, such as SVR, can be employed.

- Validate the model: Use the test dataset to evaluate the model's performance. Assess metrics such as accuracy and precision values to determine the effectiveness of the model.

The data acquitition was carried out in a paddy field of the Ciherang variety located at Ciawitali, North Cimahi, West Java, Indonesia (-6.8663041, 107.5514779) in August 2021, and 49 paddy plants were planted in pots that were treated with different fertilizing levels in November 2021. The data were collected during the panicle initiation about 60-70 days after transplantationThis is a critical period in rice growth when the number of potential grain-bearing tillers is determined and rice plants have a high demand for N uptake [23], also known as the highest NDVI value of the rice at the transition from the vegetative to reproductive phase [24].

A. Data and Image Collection

The methodology for the field measurements is covered in this section, in which each dataset consists of SPAD values, multispectral images (RE and OCN), image captured time, and light intensity. According to reference [25], the fourth fully open leaf from the top, located at a position 1/3 from the tip to the base of the rice leaf, is considered the most suitable for predicting the nitrogen content of rice plants. The process of measuring the SPAD value using the SPAD meter is illustrated in Fig. 1.

Fig. 1. Measuring the SPAD value on the fourth leaf 1/3 from the tip.

To obtain accurate ground truth data with a uniform distribution of rice N content, two types of SPAD measurements were performed. First, measurements were taken in the rice fields on August 19, 2021. The SPAD values were measured three times on six to ten tillers of each 36 rice plant. Second, the SPAD values were measured from 49 rice plants planted in pots on November 6, 16 and 20, 2021. The SPAD values were measured three to five times on eight to ten tillers.

The multispectral image acquisitions are carried out on the same rice plants as the SPAD data measurements. The experiments have revealed key considerations in capturing images, including the avoidance of shadows on the leaves under analysis and ensuring that the camera was perpendicular to the field. To illustrate the impact of shades on rice leaves, Fig. 2 showcases a visual representation. The OCN image in which the leaf was shaded led to an enlargement of the NDVI value in the corresponding area, indicated by a darker greenness (pointed by the arrows sign). On the other hand, Fig. 3 demonstrates an exemplary multispectral image captured from an appropriate camera angle, devoid of any shadows. These issues also should be considered when capturing the RE image.

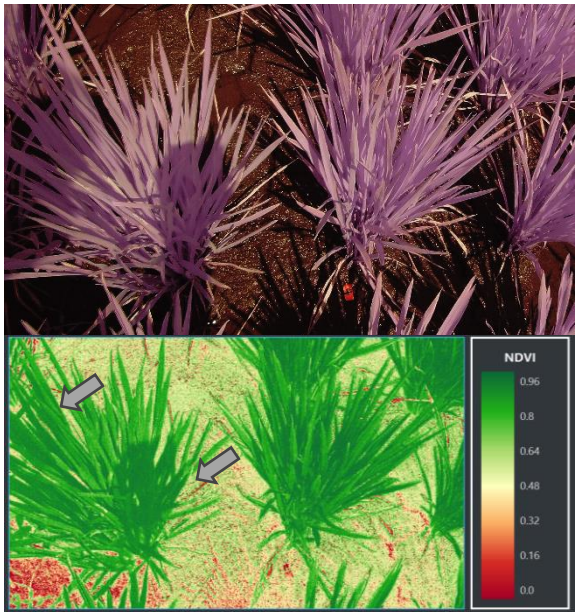

Fig. 2. Impact of shadow on NDVI value.

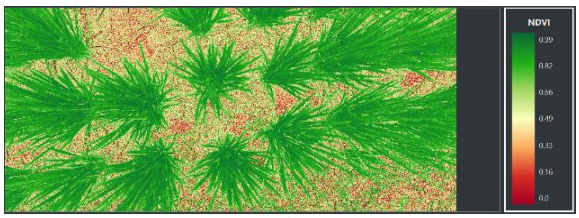

Fig. 3. Example of the correct image.

Table I further demonstrates the impact of visual light intensity on the NDVI value. The measurement of light intensity was performed using the GY1145 sensor module, which is capable of quantifying both visible and infrared light. The resulting measurement is obtained as a numerical value derived from the internal 16-bit analog-to-digital converter. To mitigate the influence of these aspects, image capture was conducted between 10:00 and 14:00 hours to minimize the presence of shadows. Additionally, the camera was positioned vertically above the rice plants to ensure consistency, and concurrent light intensity measurements were taken as an additional feature for the dataset. It is worth noting that the height of the camera during image capture, approximately ranging between 100 to 140cm, did not yield any discernible impact on the NDVI and RE calculation results.

Table I. Data on the impact of visual light intensity on the NDVI value.

Rice plant number	Visible light intensity	Calculated NDVI value
7	1894	0.58796
7	1844	0.60607
7	1852	0.60362
7	1447	0.61758
7	1260	0.71443
7	1161	0.75339
7	1085	0.78573

Furthermore, there are two aspects related to the use of the MAPIR Survey3W OCN and RE cameras that need to be considered: proper exposure settings and radiometric calibration. The user instructions recommend manual settings with a combination of ISO and shutter speed to achieve the correct exposure. The changing light intensity in the field often needs to adapt to these. Therefore, in this research, an ISO is fixed to 50 (due to capturing images during high-light intensity daylight), and the shutter speed setting depends on the light intensity. MAPIR provides tools for radiometric calibration using the MAPIR Reflectance Calibration Target (MRCT), which consists of four calibration targets with known reflectance values as shown in Fig. 4 [26].

Fig. 4. MAPIR Reflectance Calibration Target in OCN image.

MAPIR also offers an application to process and calibrate the collected images based on the MRCT images. Thus, in this research, the MRCT images need to be captured first before capturing the rice images to ensure obtaining images with accurate reflectance. The rice multispectral images were captured three to six times from slightly different angles, at the same times the captured time were recorded. At this step, each data pair consists of OCN and RE images, visible light intensity, IR light intensity, image captured time, and SPAD value.

B. Data Cleaning and Image Preprocessing

In practical implementation, SPAD values may not be consistently identical among different leaves on a single rice plant, and variations in SPAD readings can even occur at the same leaf measurement point. To address this variability, measurements are taken as described in Section A. This generates a substantial amount of data that requires careful selection. The

data-cleaning process for SPAD involves the application of Tukey's method for identifying outliers [27]. Outlying data points beyond the established boundaries are eliminated from the dataset.

The captured OCN and RE images are in a pair of RAW and JPG formats. Using the Mapir Camera Control (MCC) application and pressing the "Analyze" button will automatically detect the camera model and filter type. Subsequently, it evaluates the exposure and verifies the availability of an MRCT image that meets the specified requirements, as shown in Fig. 5.

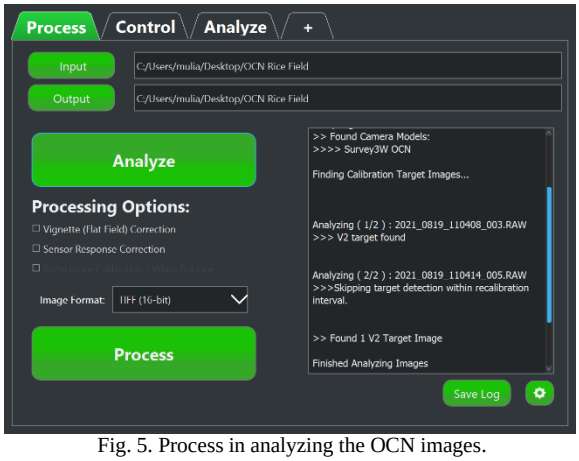

Fig. 5. Process in analyzing the OCN images.

The next step, after selecting options for vignette correction, sensor response correction, and reflectance calibration, is to press the "Process" button to convert, correct, and calibrate RAW format images into 16-bit TIFF format images, as depicted in the dialog box shown in Fig. 6. The resulting conversions are then grouped based on the rice plant to facilitate subsequent data processing.

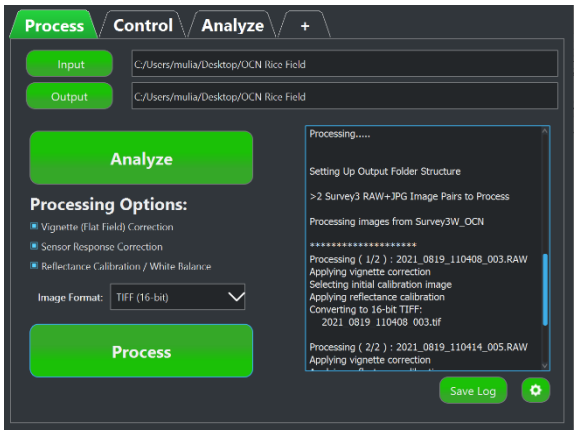

Fig. 6. Process in correction and calibration.

The calibrated images are subsequently manually cropped to eliminate undesired objects and backgrounds that may interfere with the calculation of reflectance values. The criteria for selecting regions to be cropped include rice plants within the designated individual rice plants corresponding to the moment of SPAD value measurement. An example of cropping applied to the rice planted in the field, both for OCN and RE images, is illustrated in Fig. 7 and Fig. 8, respectively.

Fig. 7. Apply cropping to the OCN image.

Fig. 8. Apply cropping to the RE image.

The cropped image will be segmented using the thresholding method to separate the rice leaf from its surrounding background, such as water and soil. Shadowed leaves should also be filtered out when determining the threshold value. An example of reflectance values is shown in Fig. 9.

Fig. 9. Reading the reflectance value.

Upon examining the NIR reflectance values of multiple brightly colored leaves, the leaf's NIR reflectance value is determined by taking the lowest value; the resulting value of 8825 was obtained. After reading the NIR reflectance values of a few background pixels, the greatest value is chosen to represent the background NIR reflectance value, giving 5614. The threshold value of 7219.5, rounded to 7200, is determined by applying Eq. (1). To find the

threshold value for RE image segmentation, the same process was followed, and the result was 7500. Figure 10 shows an example of segmentation results for the OCN and RE images.

$$Thr = BackR + (LeafR - BackR)/2 \quad (1)$$

, where *Thr* is the threshold value, *BackR* is the background NIR reflectance, and *LeafR* is the leaf NIR reflectance.

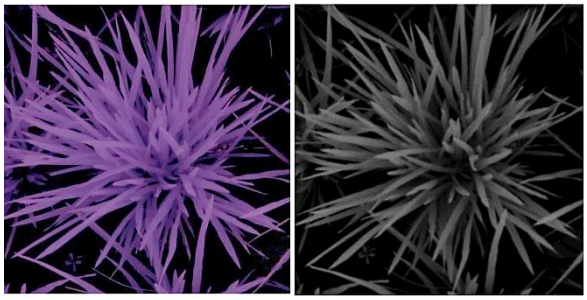

Fig. 10. Image segmentation result.

C. Retrieve Spectral Data

The most common and widely used VI in remote sensing for determining vegetation health and vigor is the NDVI [28]. Although it does not directly measure N content in plants, some research has found a strong correlation between NDVi value and N content in plants, including rice [29, 30]. The reason for using NDVI in determining N content also can be examined based on Eq. (2), and a quantitative approach provides a means to analyze large-scale patterns and trends in vegetation health.

$$NDVI = (NIR - R)/(NIR + R) \quad (2)$$

, where *NDVI* is the NDVI calculated value, *NIR* is the NIR reflectance, and *R* is the red reflectance.

Chlorophyll strongly absorbs red light and reflects near-infrared light. Healthy, chlorophyll-rich vegetation tends to exhibit high NDVI values. Since chlorophyll is closely linked to N content, NDVI can indirectly indicate the presence and health of chlorophyll, thereby relating to N levels. However, NDVI has drawbacks, being sensitive to background factors such as brightness and shadows on leaves, as well as soil brightness [31]. In this study, these two issues have been anticipated by employing segmentation and using the OCN filter on MAPIR Survey3W camera.

NDVI is calculated for each pixel, and varied NDVI values are obtained in a single image. To clean the data from outliers, Tukey's method is employed. Subsequently, the average NDVI values for the image are calculated. The purpose of calculating the average NDVI value is to obtain a single NDVI value representing the image. The NDVI image can be seen in Fig. 11, which also shows the background pixel (718, 297) with no NDVI value, while the leaf pixel (1007, 965) has an NDVI value of 0.4181. The same rice plant with different view angles may cause slightly different NDVI values. Due to their underexposure, 132 datasets that were obtained on November 20 were unable to be calibrated and converted. So at this stage, there are a total of 540 data pairs consisting of features of visible light intensity, IR light intensity, NDVI value, RE value, image captured time, and SPAD value as the label (output).

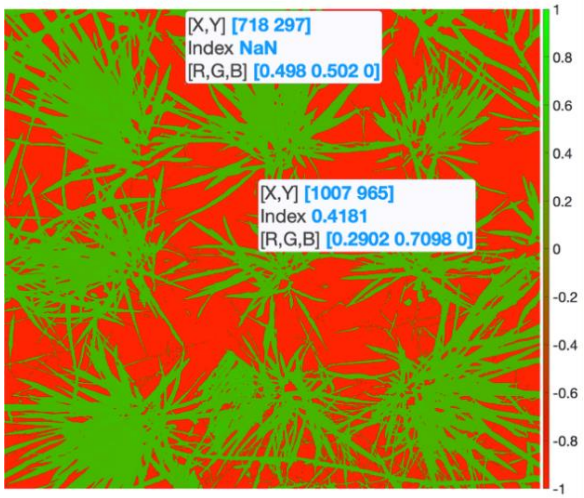

Fig. 11. Calculated NDVI value.

D. Develop A Prediction Model

In constructing predictive models for estimating N content, various machine-learning algorithms are often employed, particularly when dealing with nonlinear data [21, 32]. One workable algorithm commonly utilized for N estimation in rice is the SVR [33, 34, 35]. Thus, this research adopts SVR to develop a predictive model. Before using the obtained dataset to build the SVR model, it is necessary to examine the correlations based on the acquisition date as shown in Table II.

Table II. Correlation test.

Date	No. of data	Pearson test	Canova test
19 August	137	0.332	0.545
6 November	144	0.542	0.020
16 November	143	0.181	0.500
20 November	116	0.041	0.652

The outcome shows that the datasets on August 19, November 16, and November 20 have moderate nonlinear correlations. This resulted in 396 datasets in all, which would be used to construct the prediction model. The acquired dataset was separated using Holdout Validation, allocating 10% of the data for testing performance, 10% for validation data, which serves the purpose of parameter tuning and kernel selection, and 80% for training data. The dataset split was performed randomly using the scikit-learn library. Following the division of the dataset into three segments, feature scaling was conducted to prevent one feature from dominating the others. The chosen method for feature scaling was standardization. Subsequently, a machine learning model for predicting rice nitrogen content was developed from the standardized dataset, employing the SVR algorithm.

The kernel plays a crucial role in shaping the model. The scikit-learn library provides several kernels, namely Radial Basis Function (RBF), linear, poly, and sigmoid. Table III shows the coefficient of determination (R2) values for these kernels using the command regr.score(). A higher R2 value indicates a stronger fit for a model. Based on these results, it can be concluded that the RBF kernel exhibits the best performance, with the highest score on the validation data of 0.788.

Table III. R2 of RBF, linear, poly, and sigmoid kernel.

Kernel	R2 of train data	R2 of validation data
RBF	0,704	0,788
Linear	0,465	0,696
Poly	0,518	0,589
Sigmoid	-47,2	-39,29

Furthermore, tuning was performed on the epsilon parameter through trial and error using the RBF kernel and default gamma values. The R2 results for various epsilon values are presented in Table IV, indicating that the optimal R2 for both training and validation data is achieved with an epsilon value of 0.1.

Table IV. R2 of several epsilon values.

Epsilon	R^2 of train data	R^2 of validation data
0.1 (default)	0,704	0,788
2	0,291	0,370
1	0,594	0,735
0.12	0,704	0,783
0,15	0,704	0,777
0,17	0,704	0,775
0,2	0,705	0,776
0,01	0,698	0,807

In the same way, testing was done on the gamma parameter, as Table V illustrates. The results of the trials that were run indicate that when the gamma value rises, the R2 for the training data likewise rises. However, there comes a point at which the gamma value is exceeded, beyond which the validation data score begins to decline, indicating the presence of overfitting. Consequently, a gamma value of 1.24 is used for this predictive model.

Table V. R2 of several gamma values.

Gamma	R2 of train data	R2 of validation data
0.25 (Default)	0,704	0,788
1	0,839	0,844
1,24	0,850	0,841
1,5	0,862	0,833
1,75	0,872	0,826
2	0,881	0,816
5	0,933	0,701
10	0,951	0,616
20	0,96	0,465

From the conducted experiments, the best validation data score was obtained with a gamma value of 1.24 and an epsilon value of 0.1. With these two parameters, the training data achieves an R2 of 0.850, and the validation data achieves an R2 of 0.841.

E. Validate The Model

A prediction model's performance can be assessed by comparing the SPAD prediction results with the actual SPAD values using scatter plots, mean absolute deviation (MAD), mean absolute percentage error (MAPE), root mean square error (RMSE), and coefficient determination (R2). Forty unseen test datasets were initially separated and are used to create the scatter plot shown in Fig. 12. Red dots represent the actual SPAD values, while blue dots indicate the predicted SPAD values from the constructed model.

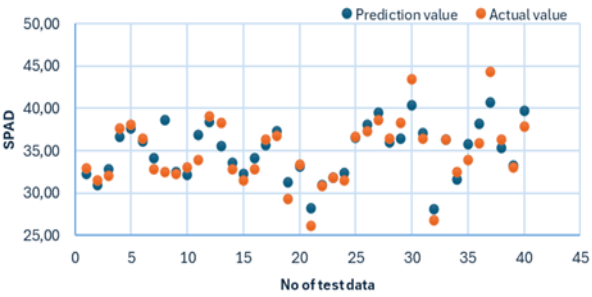

Fig. 12. The scatter plot of the prediction results.

The model prediction was illustrated in the comparison plot between the actual SPAD value on the x-axis and the predicted SPAD value on the y-axis in Fig. 13 with an R2 of 0.793. The calculated performance evaluations are MAD = 1.21, MAPE = 3.49%, and RMSE = 1.70.

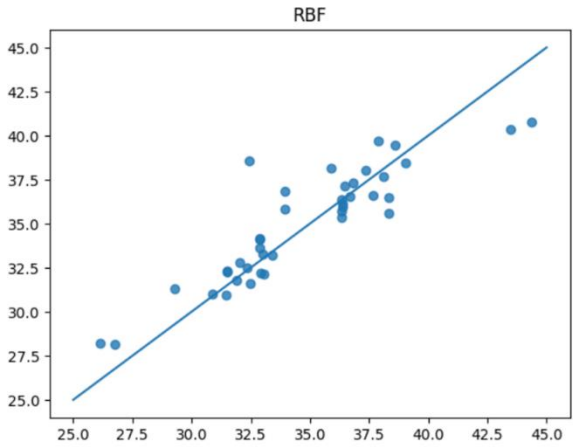

Fig. 13. The prediction results for the SPAD value with gamma 1.24 and epsilon 0.1.

III. RESULTS AND DISCUSSION

The prediction model R2 exhibits a good capacity to approximate the actual data, as evidenced by the performance evaluation for both the validation and test datasets; less than 20% of the variability in the outcome data cannot be explained by the model. The MAPE value of less than 3.5% indicates high accuracy of the prediction model, and the RMSE value of 1.70 in the SPAD measurement is also acceptable since a contact handheld chlorophyll meter on the market has a ± 1.0 to ± 3.0 SPAD accuracy. The SPAD values for rice typically range between 25 and 45, with an

optimized value of 37.5 based on [36]. This implies an RMSE% of 8.5% for this study. Comparing to the methods in N rice content prediction using UAV and multi-sensor multispectral cameras in the research [37] and [38], which have R2 of 0.68, RMSE of 11.45%, and R2 of 0.76, RMSE of 10.33%, respectively, this research offers a better result and the potential for field implementation. The model tends to forecast incorrectly for SPAD values larger than 40 or smaller than 27.5, according to scatter plot observations. This could be because there isn't much field training data available for these values. The dataset on November 6 has a low correlation and needs further analysis while data acquisition is conducted.

IV. CONCLUSION

The proposed methodology framework is capable of generating a good predictive model suitable for SSNM purposes. Further development is needed, particularly in terms of dataset expansion, especially at SPAD values smaller than 27.5 and greater than 40. Considering the limitation of the prediction model only applied to the panicle initiation stage, image acquisition collected manually, and the long processing works can be improved in future research.

ACKNOWLEDGEMENT

The authors gratefully acknowledge Universitas Kristen Maranatha for providing the facilities, and equipment for this research.

REFERENCES

[1] O. Calicioglu, A. Flammini, S. Bracco, L. Bellù and R. Sims, 'The Future Challenges of Food and Agriculture: An Integrated Analysis of Trends And Solutions,' *Sustain.*, vol. 11, no. 1, pp. 1-21, 2019.

[2] D. Laborde, W. Martin, J. Swinnen and R. Vos, 'COVID-19 Risks to Global Food Security,' *Sci.*, vol. 369, no. 6503, pp. 500–502, 2020.

[3] H. I. Lin, Y. Y. Yu, F. I. Wen and P. T. Liu, 'Status of Food Security in East and Southeast Asia and Challenges of Climate Change', *Climate*, vol. 10, no. 3, pp. 40, 2022.

[4] S. Yuan *et al.*, 'Southeast Asia Must Narrow Down The Yield Gap to Continue to be A Major Rice Bowl,' *Nat. Food*, vol. 3, no. 3, pp. 217–226, 2022.

[5] D. K. Ray, N. D. Mueller, P. C. West and J. A. Foley, 'Yield Trends Are Insufficient to Double Global Crop Production by 2050,' *PLoS One*, vol. 8, no. 6, pp. e66428, 2013.

[6] B. Singh and V. K. Singh, 'Fertilizer Management in Rice,' in B. S. Chauhan, K. Jabran, and G. Mahajan, *Rice Production Worldwide*, Springer, pp. 217–253, 2017.

[7] B. Wang, G. Zhou, S. Guo, X. Li, J. Yuan and A. Hu, 'Improving Nitrogen Use Efficiency in Rice for Sustainable Agriculture: Strategies and Future Perspectives,' *Life*, vol. 12, no. 10, pp. 1–13, 2022.

[8] P. Chivenge, S. Sharma, M. A. Bunquin and J. Hellin, 'Improving Nitrogen Use Efficiency—A Key for Sustainable Rice Production Systems,' *Front. Sustain. Food Syst.*, vol. 5, no. November, pp. 737412, 2021.

[9] A. Dass, V. K. Suri and A. K. Choudhary, 'Site-specific Nutrient Management Approaches for Enhanced Nutrient-Use Efficiency in Agricultural Crops,' *J. Crop Sci. Technol.*, vol. 3, no. 3, pp. 1–6, 2014.

[10] Y. P. Wang, Y. C. Chang and Y. Shen, 'Estimation of Nitrogen Status of Paddy Rice at Vegetative Phase Using Unmanned Aerial Vehicle Based Multispectral Imagery,' *Precis. Agric.*, vol. 23, no. 1, pp. 1–17, 2022.

[11] H. Zheng, T. Cheng, D. Li, X. Zhou, X. Yao, Y. Tian, W. Cao and Y. Zhu, 'Evaluation of RGB, Color-Infrared and Multispectral Images Acquired from Unmanned Aerial Systems for The Estimation of Nitrogen Accumulation in Rice,' *Remote Sens.*, vol. 10, no. 6, pp. 824, 2018.

[12] L. Silva, L. A. Conceição, F. C. Lidon and B. Maçãs, 'Remote Monitoring of Crop Nitrogen Nutrition to Adjust Crop Models: A Review,' *Agric.*, vol. 13, no. 4, pp. 835, 2023.

[13] M. Muliady, L. Tien Sze, K. Voon Chet and S. Patra, 'Classification of Rice Plant Nitrogen Nutrient Status Using k-Nearest Neighbors (k-NN) with Light Intensity Data,' *Indonesia. J. Electr. Eng. Comput. Sci.*, vol. 22, no. 1, pp. 179-186, 2021.

[14] M. K. Mosleh, Q. K. Hassan and E. H. Chowdhury, 'Application of Remote Sensors in Mapping Rice Area and Forecasting Its Production: A Review,' *Sensors*, vol. 15, no. 1, pp. 769–791, 2015.

[15] K. Yu, F. Li, M. L. Gnyp, Y. Miao, G. Bareth and X. Chen, 'Remotely Detecting Canopy Nitrogen Concentration and Uptake of Paddy Rice in The Northeast China Plain,' *ISPRS J. Photogramm. Remote Sens.*, vol. 78, no. April, pp. 102–115, 2013.

[16] W. S. Lee, V. Alchanatis, C. Yang, M. Hirafuji, D. Moshou and C. Li, 'Sensing Technologies for Precision Specialty Crop Production,' *Comput. Electron. Agric.*, vol. 74, no. 1, pp. 2–33, 2010.

[17] Y. C. Tian, K. J. Gu, X. Chu, X. Yao, W. X. Cao and Y. Zhu, 'Comparison of Different Hyperspectral Vegetation Indices for Canopy Leaf Nitrogen Concentration Estimation in Rice,' *Plant Soil*, vol. 376, no. 1, pp. 193–209, 2013.

[18] D. Stavrakoudis, D. Katsantonis, K. Kadoglidou, A. Kalaitzidis and I. Z. Gitas, 'Estimating Rice Agronomic Traits Using Drone-Collected Multispectral Imagery,' *Remote Sens.*, vol. 11, no. 5, pp. 545, 2019.

[19] X. Soria, A. D. Sappa and A. Akbarinia, 'Multispectral Single-Sensor RGB-NIR Imaging: New Challenges and Opportunities,' in *Seventh Int. Conf. Image Process. Theory, Tools and Appl.*, pp. 3–8, 2017.

[20] A. P. A. Gomes, D. M. De Queiroz, D. S. M. Valente, F. D. A. D. C. Pinto and J. T. F. Rosas, 'Comparing A Single-Sensor Camera with a Multisensor Camera for Monitoring Coffee Crop Using Unmanned Aerial Vehicles,' *Precisi. Agric.*, vol. 4430, pp. 87–97, 2021.

[21] A. Chlingaryan, S. Sukkarieh and B. Whelan, 'Machine Learning Approaches for Crop Yield Prediction and Nitrogen Status Estimation in Precision Agriculture: A Review,' *Comput. Electron. Agric.*, vol. 151, no. May, pp. 61–69, 2018.

[22] MAPIR, 'OCN Filter Improves Results Compared to RGN Filter'. [Online] Available: https://www.mapir.camera/pages/ocn-filter-improves-contrast-compared-to-rgn-filter.

[23] Y. Liu, X. Zhu, X. He, C. Li, T. Chang, S. Chang, H. Zhang and Y. Zhang, 'Scheduling of Nitrogen Fertilizer Topdressing During Panicle Differentiation to Improve Grain Yield of Rice With A Long Growth Duration,' *Sci. Rep.*, vol. 10, no. 1, pp. 1–10, 15197, 2020.

[24] A. A. Aguilar, 'Machine Learning and Big Data Techniques for Satellite-Based Rice Phenology Monitoring,' MPhil. Thesis, the University of Manchester, 2019.

[25] Z. Yuan, Q. Cao, K. Zhang, S. T. Ata-Ul-Karim, Y. Tian, Y. Zhu, W. Cao and X. Liu, 'Optimal Leaf Positions for SPAD Meter Measurement in Rice,' *Front. Plant Sci.*, vol. 7, pp. 1–10, 00719, 2016.

[26] MAPIR, 'Calibration Target'. [Online]. Available: https://mapir.gitbook.io/mapir-camera-control-mcc/calibration-targets.

[27] S. Seo, 'A Review and Comparison of Methods for Detecting Outliers in Univariate Data Sets,' MSc Thesis, University of Pittsburgh, 2006.

[28] L. Wang, Y. Duan, L. Zhang, T. U. Rehman, D. Ma and J. Jin, 'Precise Estimation of NDVI With A Simple NIR Sensitive RGB Camera and Machine Learning Methods for Corn Plants,' *Sensors*, vol. 20, no. 11, pp. 1–15, 2020.

[29] T. Liu, R. Li, X. Zhong, M. Jiang, X. Jin, P. Zhou, S. Liu, C. Sun and W. Guo, 'Estimates of Rice Lodging Using Indices Derived from UAV Visible and Thermal Infrared Images,' *Agric. For. Meteorol.*, vol. 252, pp. 144–154, 2018.

[30] N. N. C. Ya, L. S. Lee, M. R. Ismail, S. M. Razali, N. A. Roslin and M. H. Omar, 'Development of Rice Growth Map Using The Advanced Remote Sensing Techniques,' *Proc. 2019 Int. Conf. Comput. Drone Appl.*, vol. 2018, pp. 23–28, 2019.

[31] J. Xue and B. Su, 'Significant Remote Sensing Vegetation Indices: A Review of Developments and Applications,' *J. Sensors*, vol. 2017, pp. 1353691, 2017.

[32] H. Lee, J. Wang and B. Leblon, 'Using Linear Regression, Random Forests, and Support Vector Machine with Unmanned Aerial Vehicle Multispectral Images to Predict Canopy Nitrogen Weight in Corn,' *Remote Sens.*, vol. 12, no. 13, pp. 2071, 2020.

[33] K. K. Paidipati, C. Chesneau, B. M. Nayana, K. R. Kumar, K. Polisetty and C. Kurangi, 'Prediction of Rice Cultivation in India—Support Vector Regression Approach with Various Kernels for Non-Linear Patterns,' *AgriEngineering*, vol. 3, no. 2, pp. 182–198, 2021.

[34] L. Wang, X. Zhou, X. Zhu and W. Guo, 'Estimation of Leaf Nitrogen Concentration in Wheat using The MK-SVR Algorithm and Satellite Remote Sensing Data,' *Comput. Electron. Agric.*, vol. 140, pp. 327–337, 2017.

[35] L. Wang, Q. Chang, J. Yang, X. Zhang and F. Li, 'Estimation of Paddy Rice Leaf Area Index Using Machine Learning Methods Based on Hyperspectral Data from Multi-Year Experiments,' *PLoS One*, vol. 13, no. 12, pp. 1–16, 2018.

[36] M. Ghosh, D. K. Swain, M. K. Jha, V. K. Tewari and A. Bohra, 'Optimizing Chlorophyll Meter (SPAD) Reading to Allow Efficient Nitrogen Use in Rice And Wheat Under Rice-Wheat Cropping System in Eastern India,' *Plant Prod. Sci.*, vol. 23, no. 3, pp. 270–285, 2020.

[37] S. Xu, X. Xu, Q. Zhu, Y. Meng, G. Yang, H. Feng, M. Yang, Q. Zhu, H. Xue and B. Wang, 'Monitoring Leaf Nitrogen Content in Rice Based on Information Fusion of Multi-Sensor Imagery from UAV,' *Precis. Agric.*, vol. 24, no. 6, pp. 2327–2349, 2023.

[38] W. Wang, Y. Wu, Q. Zhang, H. Zheng, X. Yao, Y. Zhu, W. Cao and T. Cheng, 'AAVI: A Novel Approach to Estimating Leaf Nitrogen Concentration in Rice from Unmanned Aerial Vehicle Multispectral Imagery at Early and Middle Growth Stages,' *IEEE J. Sel. Top. Appl. Earth Obs. Remote Sens.*, vol. 14, pp. 6716–6728, 2021.